Available online at www.sciencedirect.com
SCIENCE DIRECT
Polymer 46 (2005) 6201–6207
polymer
www.elsevier.com/locate/polymer

Order to disorder transition of comb copolymer $A_{m+1}B_m$: a self-consistent field study

Rong Wang*, Zhibin Jiang, Jinglei Hu

Department of Polymer Science and Engineering, College of Chemistry and Chemical Engineering, Nanjing University, Nanjing 210093, China

Received 4 November 2004; received in revised form 28 March 2005; accepted 28 March 2005
Available online 15 June 2005

Abstract

The order to disorder transition of comb copolymers $A_{m+1}B_m$ is investigated by the self-consistent field theory. Although there are only two components in a molecule, the side chain number m affects the phase diagram largely due to the fact that the architecture of a comb copolymer is not invariant under the interchange of A- with B-monomers. With the increase of the side chain number, the interaction (Flory–Huggins) parameter of the order-to-disorder transition (ODT) increases at the same composition and the lowest ODT occurs at the smaller volume fraction of the main chain f_A. The influences of the side chain density and the side chain length on the phase behavior were discussed in detail. The relation $\chi N_{ODT} \propto f_A^{\alpha}$ exists with the fixed main chain length. The comb copolymer with the large side chain number m and the long main chain sections (or short side chain) is more stable. The results are helpful to design nano- or bio-materials with complex architecture or tailor the phase behavior of comb copolymers.

Keywords: Comb copolymer; Order to disorder transition; Self-consistent field theory

1. Introduction

Comb copolymers can be composed of a long, flexible or stiff, hydrophobic backbone and dense, long or short, hydrophilic side chains that branch from this main chain. If the selective solvent is sufficiently poor for the side chains but good for the backbone, then this kind of grafted comblike copolymers is the simplest one in which both chemical and topological complexities are combined, ensuring a wide variety of different regimes of structure formation. Therefore, they are an important and interesting class of macromolecules of nonlinear global architecture. And as one particular type of amphiphiles, recent developments have demonstrated that comb-shaped polymer, where the side chains are attached to the backbone by physical interactions such as hydrogen bonding, ionic bonding, coordination complexation, etc. offer a unique concept to design functional polymeric materials [1–7].

New synthetic techniques allow synthesis of graft block copolymers having well-defined molecular architectures [8,9]. These techniques provide precise control over backbone molecular weight, arm molecular weight, arm polydispersity, the placement of the branch points along the backbone, and the number of arms grafted to each branch point. Molecules with specific, incremental backbone lengths are produced, allowing multiple grafts with well-defined architectures to be isolated and characterized.

A number of theoretical studies of chemical disorder effects are on the self-assembly behavior of polymer blends and copolymers [10–20]. Of primary interest to such investigators has been the phase behavior of AB random copolymers and AB random multiblock copolymers with different statistical models of the sequence distributions of the two types of monomers. There have also been a few investigations of AB graft copolymers where the locations of the grafting points are random variables [21–26]. Some common themes arise from these studies; specifically, that large amounts of polydispersity can lead to a competition between macrophase separation and microphase separation, delineated in some cases by Lifshitz tricritical points, and

* Corresponding author. Tel.: +86 25 8359 6802; fax: +86 25 8331 7661.
E-mail address: rong_wang73@hotmail.com (R. Wang).

0032-3861/$ - see front matter © 2005 Elsevier Ltd. All rights reserved.
doi:10.1016/j.polymer.2005.03.115

that the length scales of the mesophases are strongly temperature dependent, unlike pure block copolymer systems.

The conformational properties of single comblike macromolecules in a dilute solution have been studied by several authors using both analytical approaches [27–29] and computer simulations [30–37]. Even the structure of P(MMA-*r*-PEOM) comb polymer films and the blend of PLA/P(MMA-*r*-PEOM) at the water/polymer surface was predicted by a self-consistent field lattice model [38,39]. Almost all the previous theoretical calculation concentrated on the density profiles or the structures of the comb copolymers. Only few considerations are about the phase transitions, such as order to disorder transition, order to order transition [40,41].

In this study, we only consider the stability of the homogeneous phase relative to the microphase-separated state. The related parameters are the side chain number, m, the side chain length, the intrinsic stiffness of the backbone and the side chains. Thus, we calculate the spinodal curve in terms of the normalized Flory–Huggins parameter χN, the relative AB composition, and m, the number of teeth in the comb.

2. Calculation algorithm

We consider n comb copolymer $A_{m+1}B_m$ with polymerization N in a volume V and there are m branching points (or the side chain number) along the main chain A, which divide the main chain as $m+1$ equal parts (we called it 'divided sections') with polymerization N_A and each side chain B has N_B segments. So, $N=(m+1)N_A+mN_B$. The schematic diagram of a comb copolymer molecule is presented in Fig. 1. The monomers of the main chain and the side ones are assumed to be flexible with a statistical length a. Therefore, the compositions (average volume fractions) are $f_A=(m+1)N_A/N$, $f_B=1-f_A$ for the main chain A and the side chains B, respectively.

With the different architectures of the blocks A and B, we define four distribution functions, i.e. $q_B(\mathbf{r},s)$, $q_B^+(\mathbf{r},s,t)$, $q_A(\mathbf{r},s,t)$ and $q_A^+(\mathbf{r},s,t)$, where s is the contour along the main chain for A and along the side chain for B, t is the number along the main chain A divided by the side chains B and it belongs to $[1,m+1]$. With these definition, the polymer segment probability distributions q and q^+ for block A and block B satisfy the modified diffusion equations:

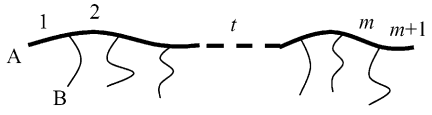

Fig. 1. Schematic representation of a comb copolymer molecule. Thick and thin lines represent main chain A and side chains B, respectively.

$$\frac{\partial}{\partial s}q=\frac{Na^2}{6}\nabla^2 q-wq \tag{1}$$

$$\frac{\partial}{\partial s}q^+=-\frac{Na^2}{6}\nabla^2 q^++wq^+ \tag{2}$$

where w is w_A when s belongs to block A, w_B when belongs to block B. The initial conditions are $q_B(\mathbf{r},0)=1$, $q_A(\mathbf{r},0,1)=1$, $q_A(\mathbf{r},0,t+1)=q_B(\mathbf{r},N_B)q_A(\mathbf{r},N_A,t)$, $q_A^+(\mathbf{r},N_A,m+1)=1$, $q_A^+(\mathbf{r},N_A,t)=q_A^+(\mathbf{r},0,t+1)q_B(\mathbf{r},N_B)$ and $q_B^+(\mathbf{r},N_B,t)=q_A(\mathbf{r},N_A,t)q_A^+(\mathbf{r},0,t+1)$, where $t\in[1,m]$. Accordingly, the partition function of a single chain subject to the mean field w_i, where i represents block species A, B, can be written as $Q=\int d\mathbf{r}q_A(\mathbf{r},N_A,m+1)$.

With above description, the free energy function (in units of k_BT) of the system is given by

$$aF=-\ln(Q/V)+1/V\int d\mathbf{r}[\chi N\phi_A\phi_B-w_A\phi_A-w_B\phi_B-\xi(1-\phi_A-\phi_B)] \tag{3}$$

where ϕ_A and ϕ_B are the monomer density of block A and B, respectively. χ is the Flory–Huggins interaction parameter between species A and B, ξ is the Lagrange multiplier (as a pressure).

Minimization of the free energy to mean field, density and pressure, $\delta F/\delta w=\delta F/\delta\phi=\delta F/\delta\xi=0$, leads to the following self-consistent field equations that describe the equilibrium state:

$$\phi_A(\mathbf{r})=\frac{V}{QN}\sum_{t=1}^{m+1}\int_0^{N_A}ds q_A(\mathbf{r},s,t)q_A^+(\mathbf{r},s,t) \tag{4}$$

$$\phi_B(\mathbf{r})=\frac{V}{QN}\sum_{t=1}^{m}\int_0^{N_B}ds q_B(\mathbf{r},s)q_B^+(\mathbf{r},s,t) \tag{5}$$

$$w_A(\mathbf{r})=\chi N\phi_B(\mathbf{r})+\xi(\mathbf{r}) \tag{6}$$

$$w_B(\mathbf{r})=\chi N\phi_A(\mathbf{r})+\xi(\mathbf{r}) \tag{7}$$

$$\phi_A(\mathbf{r})+\phi_B(\mathbf{r})=1 \tag{8}$$

Here we solve Eqs. (4)–(8) directly in real space by using a combinatorial screening algorithm proposed by Drolet and Fredrickson [42,43]. Note that one must solve the diffusion equation first for $q_B^+(\mathbf{r},s)$ with initial condition $q_B(\mathbf{r},0)=1$, then for $q_A(\mathbf{r},s,t)$ with $q_A(\mathbf{r},0,1)=1$, $q_A(\mathbf{r},0,t+1)=q_B(\mathbf{r},N_B)q_A(\mathbf{r},N_A,t)$, for $q_A^+(\mathbf{r},s,t)$ with $q_A^+(\mathbf{r},N_A,m+1)=1$, $q_A^+(\mathbf{r},N_A,t)=q_A^+(\mathbf{r},0,t+1)q_B(\mathbf{r},N_B)$ and last for $q_B(\mathbf{r},s,t)$ with $q_B^+(\mathbf{r},N_B,t)=q_A(\mathbf{r},N_A,t)q_A^+(\mathbf{r},0,t+1)$.

In this paper, we will mainly concern with the boundary of the thermodynamic instability of the homogeneous phase to a microphase-separated phase. This transition is quite generally preempted by a first-order transition. We extend the numerical version of the SCFT method to the comb copolymers. If we know the architecture of a polymer, we

can always derive the set of the self-consistent equations and the initial conditions of the modified diffusion equations.

3. Results and discussion

3.1. Phase diagram with different side chain number

We choose to consider only the lamellar structure and the hexagonal structure. By continuously changing the composition $f_A(f_B=1-f_A)$ and the Flory–Huggins parameter χ, we obtained the phase diagrams of the comb copolymer with side chain number m. The phase diagrams for comb copolymer with side chain number $m=1$, 2, 3 and 5 are shown in Fig. 2(a)–(d), respectively. The χN of the order to disorder transition (ODT) and the order to order transition (OOT) increases largely as the side chain number increases. The lamellar region seems broader with the increasing of the side chain number.

In order to compare the order to disorder transition (ODT) of the comb copolymer with different side chain number, we plot the spinodal curves in Fig. 3. Fig. 3(a) is about χN versus f_A and Fig. 3(b) is the reduced phase diagram, i.e. $\chi N/(m+1)$ versus f_A, where the solid, dash, dot, dash dot and dash dot dot lines are those of $m=1$, 2, 3, 5 and 9, respectively. As the side chain number increases, the χN of the order to disorder transition (ODT) increases largely, which corresponds to the lower temperature to microphase separate, i.e. the system becomes more stable. The minimum on the curves can be identified as the critical point. However, as the side chain number increases, the critical point shifts to values of the composition smaller than 0.5, and, thus, in contrast to a diblock, the phase diagram is not symmetric anymore. Due to m points being linked by the side chains, it is difficult for the comb copolymers to separate into hexagonal/cubic phase when $f_A \leq 0.5$. At this time, the main chains become a little stretching. The effect becomes stronger, but the difference become smaller as the side chain number m increases. Thus, we can expect that the spinodal curve will fix to the same form when the side chain number m is large.

In fact, this is a purely architectural effect, which is not present in the analogous phase diagrams of the linear multiblock copolymer $(A_nB_m)_k$ [44]. But the phase diagrams show the general shape and morphologies as expected from the literature on melts of complex block copolymers [45–48]. The asymmetry is due to the fact that the architecture of a comb copolymer is not invariant under the interchange of A- with B-monomers. The phase boundaries (see Fig. 3(a)) were elevated, which agrees with the general observation that in more complex polymer melts the disordered phase is more stable, meaning that the ODT shifts to lower temperatures as compared to the ODT of a diblock copolymer melt [48–50]. One end of the side chains and some segments of the main chain are kinked in comb copolymers. So, more complex block copolymer melts, such as comb copolymer, star polymer, will loose relatively more entropy on structure formation [50,51].

3.2. Influence of the side chain number

3.2.1. N_A and N_B fixed

Fig. 4 is the order to disorder transition curve with the fixed lengths of side chains and the main chain sections as a function of the side chain number. The reduced interaction parameter $\chi N/(m+1)$ of the order-to-disorder transition increases as the side chain number increases, which means that the comb copolymers become more stable. When the side chain length is equal to that of the main chain section, such as $N_A=15$, $N_B=15$ (triangles), the $\chi N/(m+1)$ increases linearly with the side chain number m. But for the case that the side chain length is unequal to that of the main chain section, the linearity does exist as above. When the side chain is longer than the main chain section, such as $N_A=10$, $N_B=20$ (squares) and $N_A=15$, $N_B=20$ (circles), the $\chi N/(m+1)$ is smaller than that of the case for $N_A=15$, $N_B=15$ (triangles), i.e. the equal lengths between the main section and the side chain. It is favorable for the stability of the system when side chain number m begins to increase ($m=1\rightarrow2\rightarrow3$). With m further increasing, the $\chi N/(m+1)$ of order to disorder transition ascends linearly.

When the side chain is shorter than the main chain section, such as $N_A=15$, $N_B=10$ (diamonds) and $N_A=20$, $N_B=10$ (stars), the $\chi N/(m+1)$ is larger than that of the case for $N_A=15$, $N_B=15$ (triangles). It is unfavorable for the stability of the system when side chain number m begins to increase ($m=1\rightarrow2$). With m further increasing, the curves go up. In the case, f_A is larger than 0.6, which belongs to right side in Fig. 3(b). Therefore, the $\chi N/(m+1)$ of order to disorder transition increases with the same m, which means that the larger the difference between f_A and f_A^{cr}, more stable the system.

From Fig. 4(a), we can also see that the curves are nearly superposed when $N_A=10$, $N_B=20$ (squares) and $N_A=15$, $N_B=20$ (circles). But the slope of the curve is a little larger as $N_A=15$, $N_B=10$ (diamonds) and $N_A=20$, $N_B=10$ (triangles). It is easy to understand, if we choose N_A and N_B to satisfy $f_A\in(0.35,0.65)$, the χN of order to disorder transition nearly increases in a form of geometric proportion, see Fig. 3(a). But, when the lengths of the main chain sections and the side chains are different largely, the volume fractions of the main chain or the side chains f_A or $f_B<0.35$, which means that the χN of order to disorder transition increases larger and larger with increasing of the side chain number.

Fig. 4(b) is the order to disorder transition curve with the fixed lengths of side chains and the main chain sections as a function of the volume fraction of the main chain converted from the side chain number, i.e. $f_A=(m+1)N_A/((m+1)N_A+mN_B)$. From the figure, we can clearly see that the behavior of the order-to-disorder transition is different

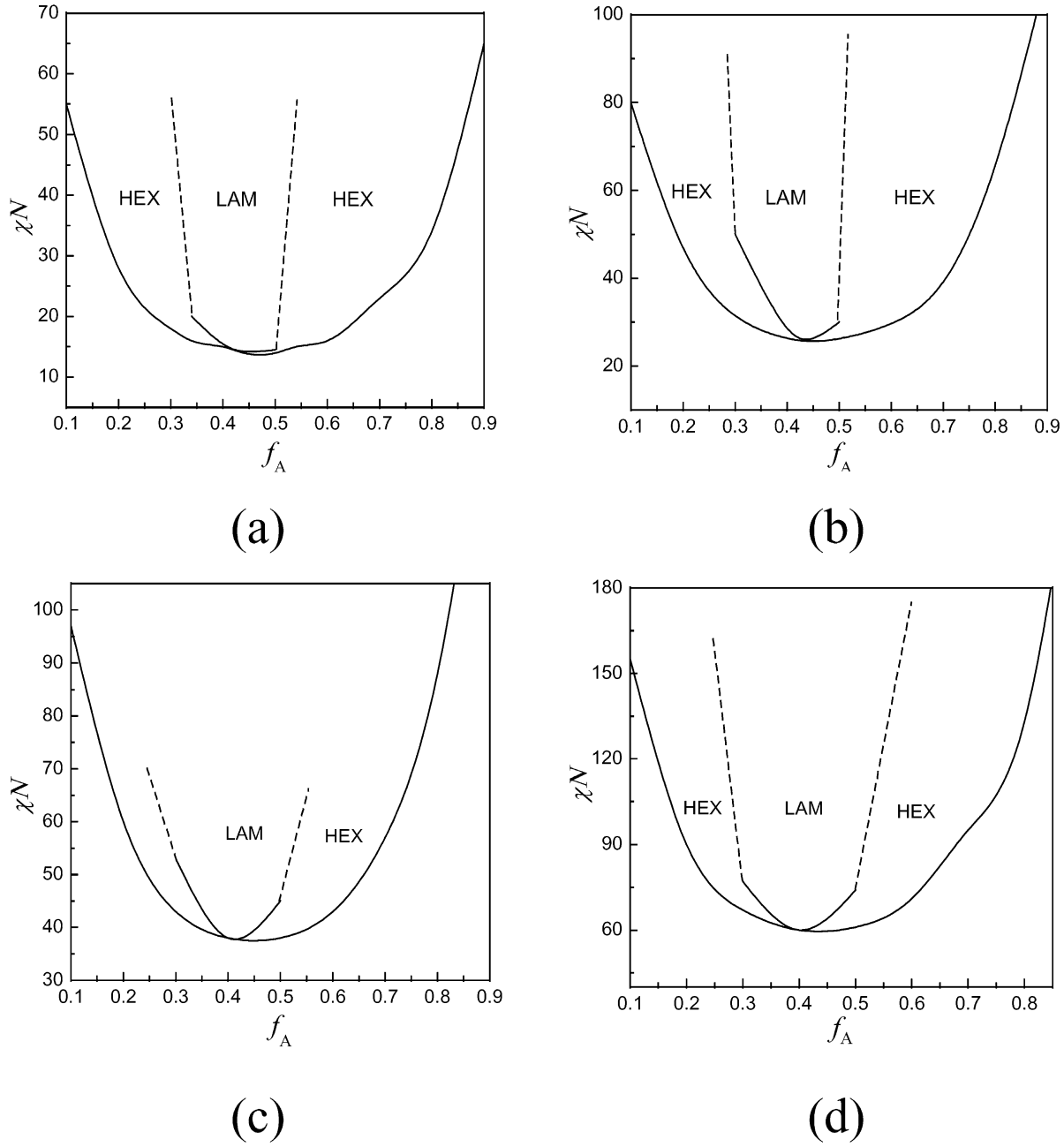

Fig. 2. Phase diagram for comb copolymer with different side chain number. (a) $m=1$; (b) $m=2$; (c) $m=3$; (d) $m=5$.

largely between the ratio ($\lambda=N_A/N_B$) of the lengths of the main chain section and the side chain. The volume fraction of the main chain f_A decreases nearly to a constant with the side chain number increasing. But the χN of the order-to-disorder transition increases largely. Therefore, the curves become sharp when the side chain number is large, especially for $\lambda>1$. Comparing these curves, we can conclude that the comb copolymers are more stable at shorter side chain and larger side chain number.

3.2.2. $(m+1)N_A$ fixed

There is another case that the side chain number will influence the order to disorder transition behavior. If the main chain length is fixed, the transition behavior will change largely as the side chain number increases, i.e. the side chain density increases. Fig. 5 is the curves of the order-to-disorder transition with different side chain number at the fixed main chain length $(m+1)N_A=120$, where we change the horizontal coordinate of the side chain number m to the composition $f_A=(m+1)N_A/((m+1)N_A+mN_B)$, i.e. $f_A=120/(120+mN_B)$ in the case. As the side chain number increases, the side chain density increases, and the volume fraction of the main chain f_A decrease. And the χN of the order-to-disorder transition increases as a function of f_A^{α}, i.e.

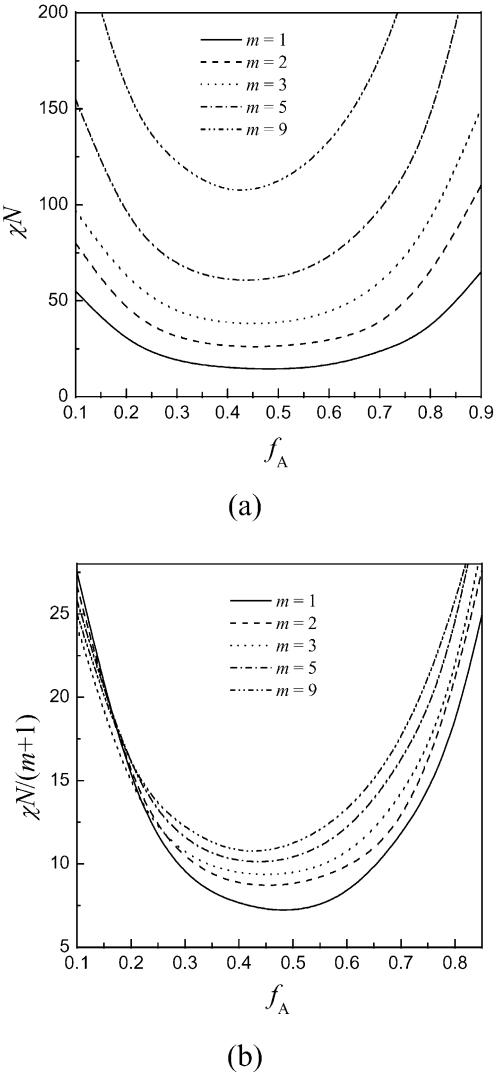

Fig. 3. The spinodal curves of the comb copolymer with different side chain number $m=1$ (solid), 2 (dash), 3 (dot), 5 (dash dot) and 9 (dash dot dot). (a) χN versus f_A; (b) $\chi N/(m+1)$ versus f_A.

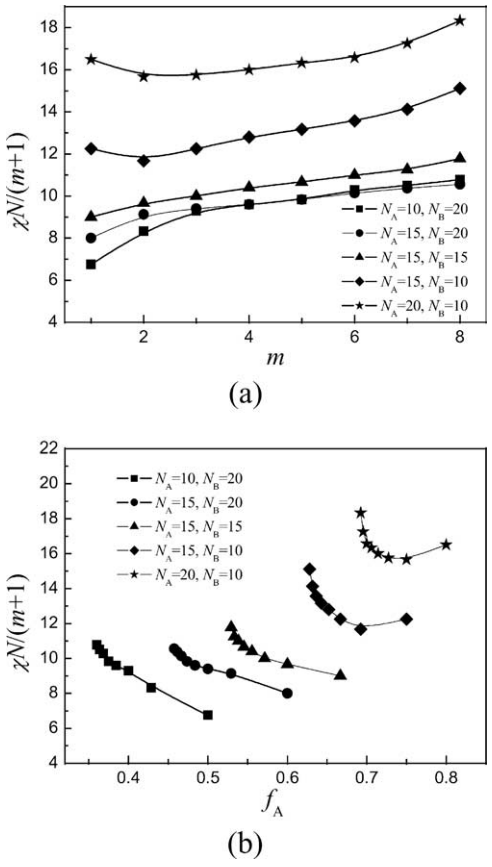

Fig. 4. Order to disorder transition curve with the fixed lengths of the main chain sections and the side chains (1) $N_A=10$, $N_B=20$ (squares), (2) $N_A=15$, $N_B=20$ (circles), (3) $N_A=15$, $N_B=15$ (triangles), (4) $N_A=15$, $N_B=10$ (diamonds), (5) $N_A=20$, $N_B=10$ (stars). (a) $\chi N/(m+1)$ versus m; (b) $\chi N/(m+1)$ versus f_A.

$\chi N_{ODT} \propto f_A^{\alpha}$ ($\alpha=-7/4$ at $(m+1)N_A=120$), which confirms that the system is more stable with the increasing of the side chain number (or density).

3.3. Influence of the side chain length

Side chain length N_B is an important variable to tailor the phase behavior of the comb copolymer. Fig. 6 is the curve of the order-to-disorder transition of the comb copolymer with the side chain number $m=5$ and the fixed main chain length $(m+1)N_A=120$, i.e. $N_A=20$, where (a) is χN versus N_B and (b) is $1/\chi$ versus f_A. When the side chain is shorter than the main chain section, χN of ODT decreases first with increasing the length of the side chain length and increases after the critical composition (f_B^{cr}). Fig. 6(b) can clearly show the relation between the ODT temperature ($T\sim 1/\chi$) and the composition at the fixed main chain length and the side chain number. It is in good agreement with the result in Ref. [41]. In this case the phase diagram is convex and, therefore, the system becomes more stable with respect to microphase separation as the difference between the composition f_B and the critical composition f_B^{cr} increases.

The absolute values of the slopes at both sides of the critical composition are different largely. The absolute value

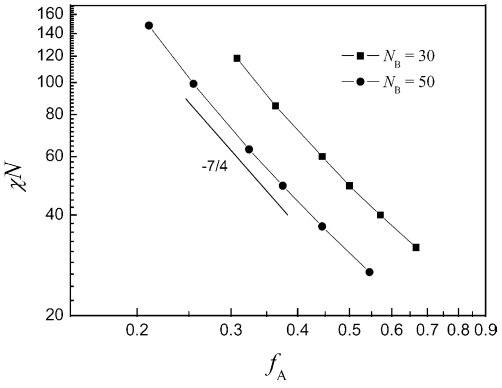

Fig. 5. Order to disorder transition curve with the fixed main chain length $(m+1)N_A=120$ and the side chain length $N_B=30$ (squares), 50 (circles), where $f_A=(m+1)N_A/((m+1)N_A+mN_B)$.

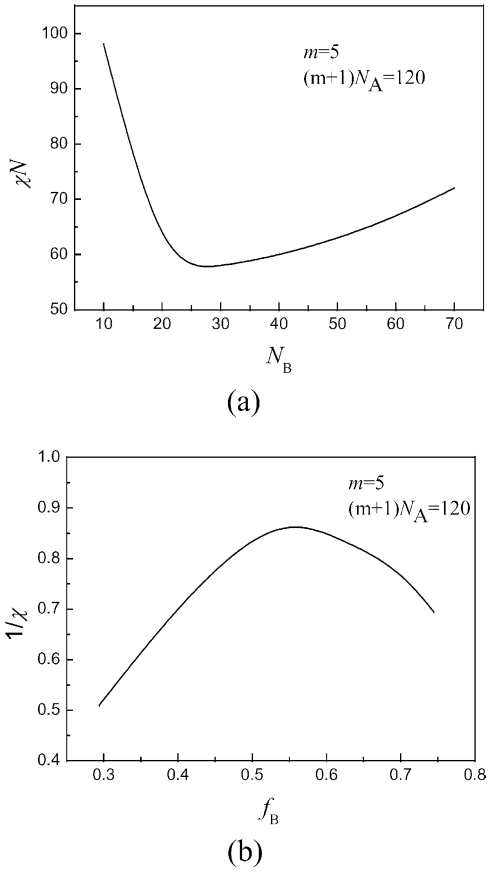

Fig. 6. Influence of side chain length (N_B) on the order-to-disorder transition with the fixed main chain length $(m+1)N_A=120$ and the side chain number $m=5$. (a) χN versus N_B, (b) $1/\chi$ versus f_A.

of the slope is larger when $f_B < f_B^{cr}$, which means that the longer main chain section is more favorable for the stability.

4. Conclusions

The numerical version of the self-consistent field theory was successfully extended to study the phase behavior of the comb copolymers. The phase diagrams become asymmetrical with the side chain number increasing, which is due to the fact that the architecture of a comb copolymer is not invariant under the interchange of A- with B-monomers. The phase boundaries were elevated with the increase of the side chain number, which agrees with the general observation that in more complex polymer melts the disordered phase is more stable, meaning that the ODT shifts to lower temperatures as compared to the ODT of a diblock copolymer melt. As the lengths of the main chain sections and the side chains are fixed, the $\chi N/(m+1)$ of the order to disorder transition increases with the side chain number increasing. But the phase behavior of the order-to-disorder transition is different largely between the ratio ($\lambda = N_A/N_B$) of the lengths of the main chain section and the side chain. And the χN of the order to disorder transition decreases with the side chain number increasing as the length of the main chain is fixed, i.e. the side chain density increases. The relation $\chi N_{ODT} \propto f_A^{\alpha}$ exists with the fixed main chain length. The χN of the order to disorder transition will decrease first, and then increase after passing through the critical value with the side chain length increasing. Altogether, the comb copolymer with the large side chain number m and the long main chain sections (or short side chain) is more stable. The results are helpful to design materials with complex architecture or tailor the phase behavior of comb copolymers.

Acknowledgements

We gratefully acknowledge financial support by National Natural Science Foundation of China (No. 20374027), Nanjing University Talent Development Foundation (No. 0205004107) and Natural Science Foundation of Nanjing University (No. 0205005216). The numerical calculations were carried out on the high-performance computers, SGI Origin 3800 and Dawning 3000A, of Nanjing University.

References

[1] Viville P, Leclere P, Deffieux A, Schappacher M, Bernard J, Borsali R, et al. Polymer 2004;45:1833–43.
[2] Jannasch P, Loyens W. Solid State Ionics 2004;166:417–24.
[3] Ikkala O, ten Brinke G. Science 2002;295:2407–9.
[4] Maki-Ontto R, de Moel K, de Odorico W, Ruokolainen J, Stamm M, ten Brinke G, et al. Adv Mater 2001;13:117–21.
[5] Kosonen H, Ruokolainen J, Knaapila M, Torkkeli M, Jokela K, Serimaa R, et al. Macromolecules 2000;33:8671–5.
[6] Thunemann AF, Lochhaas KH. Langmuir 1998;14:4898–903.
[7] Ruokolainen J, Makinen R, Torkkeli M, Makela T, Serimaa R, ten Brinke G, et al. Science 1998;280:557–60.
[8] Xenidou M, Hadjichristidis N. Macromolecules 1998;31:5690–4.
[9] Iatrou H, Mays JW, Hadjichristidis N. Macromolecules 1998;31:6697–701.
[10] Dobrynin AV, Leibler L. Macromolecules 1997;30:4756–65.
[11] Dobrynin AV, Leibler L. Europhys Lett 1996;36:283–7.
[12] Fredrickson GH, Milner ST, Leibler L. Macromolecules 1992;25:6341–54.
[13] Fredrickson GH, Milner ST. Phys Rev Lett 1991;67:835–8.
[14] Semenov AN. Eur Phys J B 1999;10:497–507.
[15] Semenov AN. Journal De Physique Ii 1997;7:1489–97.
[16] Semenov AN. Phys Rev Lett 1998;80:1908–11.
[17] Subbotin AV, Semenov AN. Eur Phys J E 2002;7:49–64.
[18] Sfatos CD, Gutin AM, Shakhnovich EI. J Phys a-Math Gen 1994;27:L411–L6.
[19] Sfatos CD, Gutin AM, Shakhnovich EI. Phys Rev E 1993;48:465–75.
[20] Sfatos CD, Shakhnovich EI. Phys Rep-Rev Sect Phys Lett 1997;288:77–108.
[21] Qi L, Lin YQ, Wang FS. Solid State Ionics 1998;109:145–50.
[22] Foster DP, Jasnow D, Balazs AC. Macromolecules 1995;28:3450–62.
[23] Shinozaki A, Jasnow D, Balazs AC. Macromolecules 1994;27:2496–502.
[24] Qi SY, Chakraborty AK, Wang H, Lefebvre AA, Balsara NP, Shakhnovich EI, et al. Phys Rev Lett 1999;82:2896–9.
[25] Qi SY, Chakraborty AK. J Chem Phys 2001;115:3401–5.

[26] Qi SY, Chakraborty AK, Balsara NP. J Chem Phys 2001;115:3387–400.
[27] Birshtein MW, Borisov OV, Zhulina EB, Khokhlov AR, Yurasova TA. Polym Sci USSR 1987;A29:1293–300.
[28] Rouault Y, Borisov OV. Macromolecules 1996;29:2605–11.
[29] Fredrickson GH. Macromolecules 1993;26:2825–31.
[30] Saariaho M, Subbotin A, Szleifer I, Ikkala O, ten Brinke G. Macromolecules 1999;32:4439–43.
[31] Saariaho M, Subbotin A, Ikkala O, ten Brinke G. Macromol Rapid Commun 2000;21:110–5.
[32] McCrackin FL, Mazur J. Macromolecules 1981;14:1214–20.
[33] Saariaho M, Ikkala O, Szleifer I, Erukhimovich I, tenBrinke G. J Chem Phys 1997;107:3267–76.
[34] Saariaho M, Szleifer I, Ikkala O, ten Brinke G. Macromol Theory Simul 1998;7:211–6.
[35] Saariaho M, Ikkala O, ten Brinke G. J Chem Phys 1999;110:1180–7.
[36] Gallache Lv, Windwer S. J Chem Phys 1966;44:1139.
[37] Lipson JEG. Macromolecules 1991;24:1327–33.
[38] Irvine DJ, Mayes AM, Griffith LG. Biomacromolecules 2001;2:85–94.
[39] Irvine DJ, Ruzette AVG, Mayes AM, Griffith LG. Biomacromolecules 2001;2:545–56.
[40] Shinozaki A, Jasnow D, Balazs AC. Macromolecules 1994;27:2496–502.
[41] Khalatur PG, Khokhlov AR. J Chem Phys 2000;112:4849–61.
[42] Drolet F, Fredrickson GH. Phys Rev Lett 1999;83:4317–20.
[43] Drolet F, Fredrickson GH. Macromolecules 2001;34:5317–24.
[44] Matsen MW, Schick M. Macromolecules 1994;27:7157–63.
[45] Delacruz MO, Sanchez IC. Macromolecules 1986;19:2501–8.
[46] Morozov AN, Fraaije J. J Chem Phys 2001;114:2452–65.
[47] Delacruz MO. Phys Rev Lett 1991;67:85–8.
[48] Marko JF. Macromolecules 1993;26:1442–4.
[49] Benoit H, Hadziioannou G. Macromolecules 1988;21:1449–64.
[50] Buzza DMA, Hamley IW, Fzea AH, Moniruzzaman M, Allgaier JB, Young RN, et al. Macromolecules 1999;32:7483–95.
[51] Matsen MW, Gardiner JM. J Chem Phys 2000;113:1673–6.